

“© 2011 IEEE. Personal use of this material is permitted. Permission from IEEE must be obtained for all other uses, in any current or future media, including reprinting/republishing this material for advertising or promotional purposes, creating new collective works, for resale or redistribution to servers or lists, or reuse of any copyrighted component of this work in other works.”

# Study on Rotational Hysteresis and Core Loss under Three Dimensional Magnetization

Yongjian Li<sup>1,2</sup>, Jianguo Zhu<sup>2</sup>, *Senior Member, IEEE*, Qingxin Yang<sup>1</sup>, Zhi Wei Lin<sup>2</sup>,  
Youguang Guo<sup>2</sup>, *Senior Member, IEEE*, and Chuang Zhang<sup>1</sup>

<sup>1</sup>Province-Ministry Joint Key Laboratory of Electromagnetic Field and Electrical Apparatus Reliability,  
Hebei University of Technology, Tianjin, 300130, China

<sup>2</sup>School of Electrical, Mechanical and Mechatronic Systems, University of Technology, Sydney, NSW 2007, Australia

In this paper, magnetic properties of soft magnetic composite (SMC) materials under alternating and various rotational magnetizations have been properly measured, modeled, and analyzed at typical frequencies of 5 Hz, 50 Hz and 500 Hz. The relationship between the magnetic flux density  $\mathbf{B}$  vector and magnetic field strength  $\mathbf{H}$  vector has been systemically studied when the  $\mathbf{B}$  loci are well controlled to be circles and ellipses in three orthogonal planes of the three dimensional (3D) tester. The core loss features against magnetic flux densities with alternating and rotational magnetizations are also compared and analyzed. It is found that the rotational core losses are nearly twice of the alternating core losses at the same magnitude of flux density. Experimental results show that SMC materials have good 3D features, and great potential for application in rotational magnetic flux machines.

*Index Terms*— Anisotropy, Core loss, 3D Rotational hysteresis, Sensing coil, Soft magnetic composite (SMC)

## I. INTRODUCTION

TO EVALUATE three dimensional (3D) magnetic properties and optimize the application of a magnetic material, the  $\mathbf{B}$ - $\mathbf{H}$  hysteresis curves and core losses need to be measured with alternating or rotational magnetic fluxes depending on the application. Experimental apparatus and techniques, such as Epstein Frames and Single Sheet Testers (SST) for measurement of magnetic properties of soft magnetic materials have been developed in the past several decades [1]-[5]. However, in a rotating electrical machine, the direction of the magnetic flux vector varies with time in the 3D space of the magnetic materials. The behavior of magnetic materials with this kind of flux, which is known as the 3D rotational flux, is quite different from that with an alternating flux [6]. Reference [7] firstly introduced a 3D magnetic property testing method and measured the behavior of grain-oriented HiB M2-H 0.30-mm sheet steel in lamination structure at 50 Hz. By using this 3D tester, a series of 3D hysteresis loci of an isotropic soft magnetic composite (SMC) material were measured under various experimental conditions [8]. To extend the excitation frequency range and improve the measurement precision, an improved 3D tester with flexible excitation coils and novel precision  $\mathbf{B}$ - $\mathbf{H}$  sensing coils was designed and constructed [9].

This paper presents the experimental magnetic properties of an SMC material, SOMALOY™ 500 [10], from 5 Hz to 1000 Hz under alternating and 3D rotational excitations. Alternating hysteresis loops and 3D vector  $\mathbf{B}$  and  $\mathbf{H}$  loci are demonstrated and compared at three typical frequencies including 5 Hz, 50 Hz and 500 Hz. Detailed comparisons of core losses against magnetic flux densities between alternating and rotational magnetizations are also analyzed. It is found that the rotational core losses are nearly twice of the alternating losses when magnitude of flux density is the same. When the material is in the 3D rotational magnetization, domain rotating and domain wall motion may cause excess loss [11].

The experimental results can also provide crucial references to evaluate the core losses and fulfill the optimization design of electrical machines and apparatus.

## II. 3D MAGNETIC PROPERTY TESTING SYSTEM

The existing 3D magnetic property measurement system consists of a tester, three high performance power amplifiers, and a digital signal processing unit with AD/DA boards driven by LabVIEW software for function generation and data acquisition. The tester, as shown in Fig. 1, mainly consists of three orthogonal square-frame yokes to guide the magnetic fluxes along the  $x$ -,  $y$ -, and  $z$ -axes, and three pairs of adjustable excitation windings wrapped around the three pairs of orthogonal magnetic core poles used to produce magnetic fields along the three axes. The overall outline of the tester is a cubic with side length of 420 mm [7]-[9].

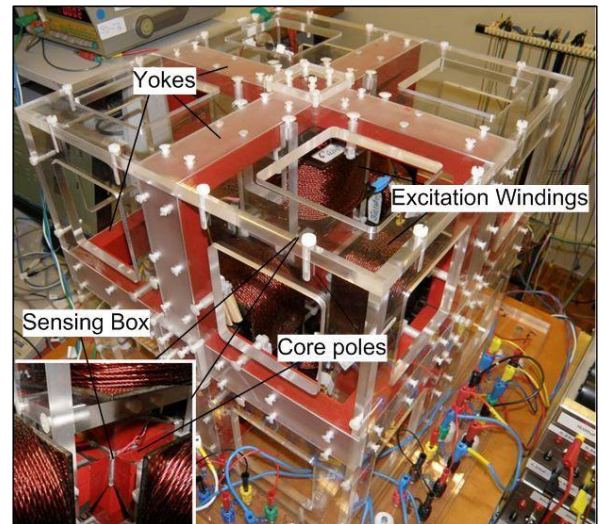


Fig. 1. Prototype of the 3-D magnetic tester.

The novel  $\mathbf{B}$ - $\mathbf{H}$  sensing coils are closely attached to the surface of a  $22 \times 22 \times 22 \text{ mm}^3$  cubic SMC specimen and

enclosed by six guarding pieces which are of the same material as the specimen. In this study, the whole sensing box with SMC specimen is mounted in the geometrical center of the tester and squeezed by six core-poles, as shown in Fig. 2. The  $\mathbf{H}$  vectors are detected by three pairs of  $H$  sensing coils and the  $\mathbf{B}$  vectors are measured by three pairs of small annular  $B$  coils, which are embedded in the  $H$  coils. Each pair of  $H$  coils or  $B$  coils on the opposite sides are connected in series and the coefficients are calibrated in detail in a long solenoid which can generate a uniform magnetic field.

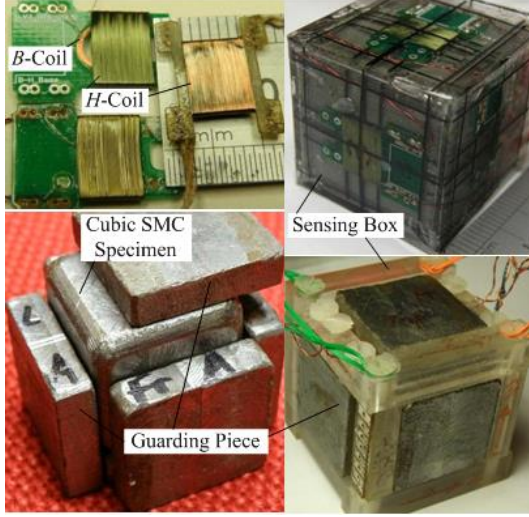


Fig. 2. Sensing box with  $B$ - $H$  coils, cubic SMC specimen and SMC guarding pieces.

The local magnetic field strength at the specimen surface depends on the position due to demagnetization factor [12], but only the field at the center of the specimen surface is relatively uniform and approximately equals to that inside the specimen. In order to improve the measurement accuracy, the size of the  $H$  sensing coil was minimized to  $8.5 \times 6 \text{ mm}^2$ . In addition, the adoption of six SMC guarding pieces ( $22 \times 22 \times 5 \text{ mm}^3$ ) can significantly improve uniformity of the magnetic field at the specimen surface, and hence improve the measurement accuracy. The comparison of the magnetic field distributions in the condition with and without SMC guarding pieces is shown in Fig. 3. This structure can also significantly decrease the equivalent reluctance of the magnetic circuit and the excitation current magnetizing the specimen.

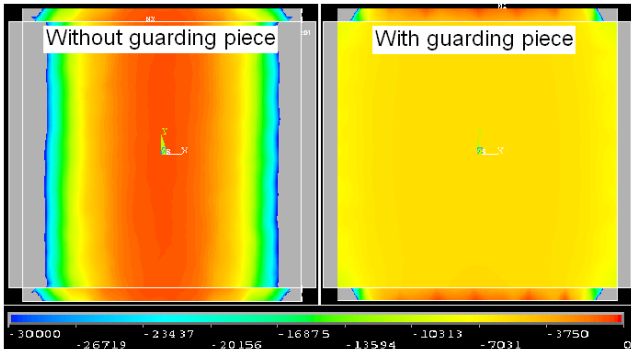


Fig. 3. Magnetic field distributions of the specimen without guarding pieces (left), and with guarding pieces (right).

### III. EXPERIMENTAL ANALYSIS AND DISCUSSION

#### A. Alternating Magnetic Properties

Alternating magnetic properties of the cubic SMC specimen were measured in the 3D tester along the  $x$ -,  $y$ -, and  $z$ -axes, respectively. Fig. 4 shows the  $\mathbf{B}$ - $\mathbf{H}$  hysteresis loops and corresponding core losses at 5 Hz, 50 Hz and 500 Hz respectively. It can be found that the hysteresis loops along  $x$ - and  $y$ -axes are very similar and slightly different from that of  $z$ -axis, in other words, the  $z$ -axis is apparent to be a hard magnetization direction. This slight anisotropy is caused by compression of iron powder during SMC synthesis and stress induced during the specimen preparation though the material is expected to be isotropy.

The average experimental core loss of the three axes is in accordance with the datasheet supplied by the material manufacturer, which also validates the 3D tester working well.

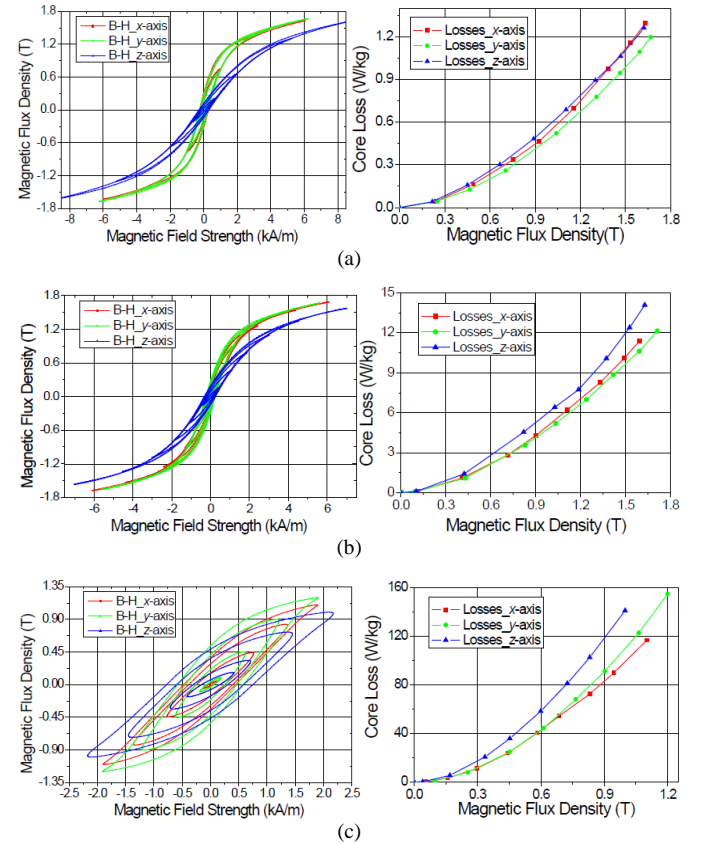


Fig. 4. Alternating hysteresis loops (left) and corresponding core losses (right) along  $x$ -,  $y$ - and  $z$ -axes at: (a) 5 Hz; (b) 50 Hz; (c) 500 Hz.

#### B. 3D Rotational Hysteresis Properties

By controlling the magnetic flux density vector  $\mathbf{B}$ , 3D rotational hysteresis properties were measured and analyzed. Various  $\mathbf{B}$  loci in the specimen, such as circle, ellipse and sphere can be obtained by adjusting phase or magnitude of sinusoidal excitation magnetic fields along three orthogonal axes. In Fig. 5, a series of well controlled circular  $\mathbf{B}$  loci in three planes and corresponding experimental  $\mathbf{H}$  loci at 5 Hz, 50 Hz and 500 Hz, are demonstrated and compared. It can be seen that the plane of the  $\mathbf{H}$  loci are nearly parallel to the corresponding well-controlled plane of the  $\mathbf{B}$  loci at 5 and 50

Hz, in other words,  $\mathbf{H}$  and  $\mathbf{B}$  loci are in the same magnetization plane at relatively lower frequencies. However, when the frequency is higher, *e.g.* 500 Hz, the  $\mathbf{B}$  and  $\mathbf{H}$  loci will not be in the same magnetization plane due to the enhanced magnetic coupling among the 3D cores. Comparing the most outer  $\mathbf{H}$  loci in the  $xoy$ -plane with loci in the  $yoz$ - and  $zox$ -planes, it is found that  $\mathbf{H}$  loci in the  $xoy$ -plane are square-like while the loci in the  $yoz$ - and  $zox$ -planes are rectangular-like. It means that  $x$ - and  $y$ -axes are relatively easier to be magnetized, which is consistent with the alternating outputs. In this cubic SMC specimen, the compression stress along the  $x$ - and  $y$ -axes is stronger than that along the  $z$ -axis. Therefore, the particles are closer and mass density is relatively high along the stronger compaction directions [13].

At low frequency, *e.g.* 5 Hz, the  $\mathbf{H}$  loci change from elliptical shape to saddle-like shape with the increasing excitation current. This change seems to be caused by the enhanced high order harmonics. The outer saddle-like  $\mathbf{H}$  locus also demonstrates that the magnetization is close to the saturation state.

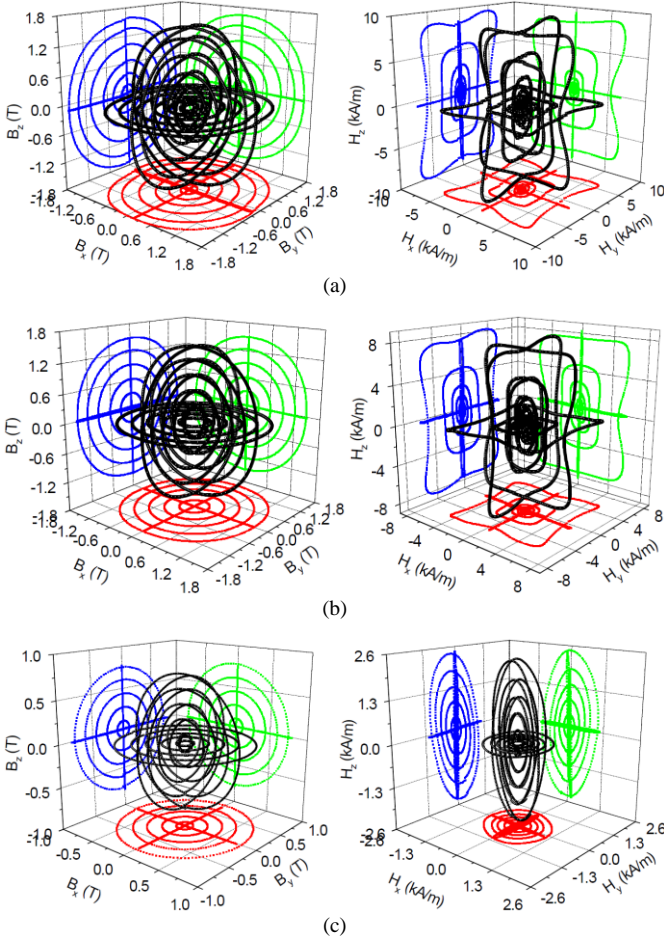


Fig. 5. Circular  $\mathbf{B}$  loci and corresponding projections in the  $xoy$ -,  $yoz$ -,  $zox$ -planes (left), and corresponding  $\mathbf{H}$  loci (right) at: (a) 5 Hz; (b) 50 Hz; (c) 500 Hz.

Fig. 6 shows a series of well controlled elliptical  $\mathbf{B}$  loci and corresponding experimental  $\mathbf{H}$  loci and projections at 50 Hz in the  $xoy$ -,  $yoz$ -, and  $zox$ -planes, respectively. The axis ratio  $\varepsilon$  (the minor axis to the major axis), is controlled from 0 to 1.

When  $\varepsilon$  is 0, it is equal to the alternating property along the major axis. Similarly, it is equal to the circularly rotational property when  $\varepsilon$  is 1. Therefore, the outermost  $\mathbf{B}$  and  $\mathbf{H}$  loci are similar with that shown in Fig. 5(b). It can be seen that  $\mathbf{B}$  and  $\mathbf{H}$  loci lie in the same magnetization planes when the  $\mathbf{B}$  loci are well controlled. Also, slight anisotropy is found in this magnetization process, and  $z$ -axis is the hard direction to be magnetized.

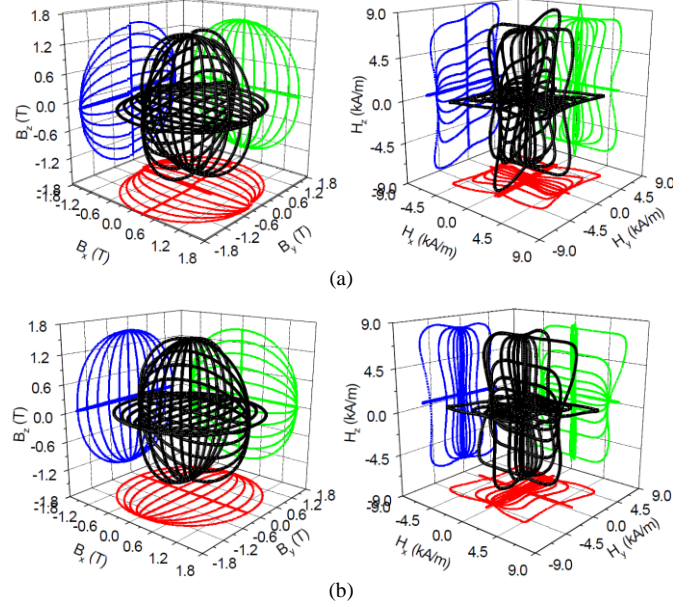


Fig. 6. Elliptical  $\mathbf{B}$  loci and corresponding projections in the  $xoy$ -,  $yoz$ -,  $zox$ -planes (left), and corresponding  $\mathbf{H}$  loci (right) at 50 Hz: (a) The axis ratio  $\varepsilon$  of the elliptical  $\mathbf{B}$  is from 0 to 1, and the major axis is  $x$ ,  $y$ , and  $z$  respectively. (b) The axis ratio  $\varepsilon$  of the elliptical  $\mathbf{B}$  is from 0 to 1, and the major axis is  $y$ ,  $z$ , and  $x$  respectively.

### C. Core Loss

Rotational core losses are calculated from the measured  $\mathbf{H}$  vectors at the specimen surface and  $\mathbf{B}$  vectors inside the specimen, which is the so-called Field-metric method [14]. This method strongly depends on the precision of measurement, which can be guaranteed by the improved sensing coils, calibration, guarding pieces, *etc.* as set forth. The total rotational core loss  $P_t$  in watts per kilogram of the specimen can be calculated in terms of the Poynting's theorem:

$$P_t = \frac{1}{T\rho_m} \int_0^T \mathbf{H} \cdot \frac{d\mathbf{B}}{dt} dt \quad (1)$$

$$= \frac{1}{T\rho_m} \int_0^T \left( H_x \frac{dB_x}{dt} + H_y \frac{dB_y}{dt} + H_z \frac{dB_z}{dt} \right) dt$$

where  $T$  is the time period of one magnetization process, and  $\rho_m$  is the mass density of the specimen.

Fig. 7 illustrates the comparison of alternating core losses and rotational core losses from 5 Hz to 1000 Hz. It is found that the rotational core losses are greater than alternating losses when magnitude of flux density is the same. For example, The rotational core losses at 5 Hz, 10Hz, 20 Hz, 50 Hz, 100 Hz, 200 Hz, 500 Hz and 1000 Hz are 0.32, 0.62, 1.18, 2.6, 7.5, 18, 67 and 162 W/kg, respectively when the magnitude of circular  $\mathbf{B}$  is 0.5 T, and the corresponding

alternating core losses are 0.18, 0.33, 0.8, 1.8, 3.8, 8.6, 30 and 82 W/kg. The rotational loss is greater (about twice) than that of alternating core loss, in particular, at higher magnetic flux densities. It is believed that the increasing loss is attributed to the domain rotating and domain wall motion, which cause the excess loss steeply increasing [11], [15].

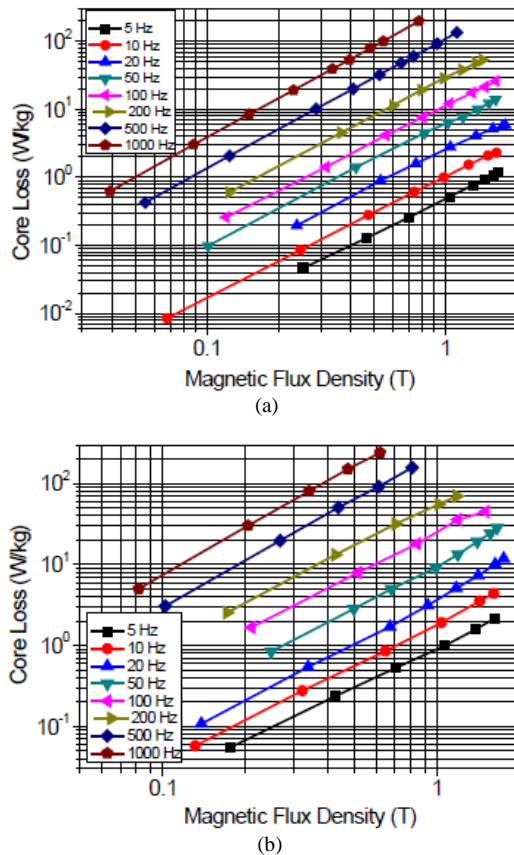


Fig. 7. Comparison of alternating core losses and rotational core losses at 5, 50 and 500 Hz: (a) Alternating core losses; (b) Rotational core losses.

#### IV. CONCLUSION

The 3D rotational hysteresis magnetic properties and corresponding core loss features were measured from 5 Hz to 1000 Hz by using the updated 3D testing system. Compared with the alternating magnetic properties at the same frequency region, the rotational core losses are greater and nearly twice that of alternating core losses due to complicated domain rotating in the testing material. Slight anisotropy is also found, which attributes to the SMC specimen preparation. In addition, the high frequency  $\mathbf{H}$  loci slightly deviate from the magnetization plane of corresponding well-controlled  $\mathbf{B}$  loci due to the enhanced magnetic coupling among the 3D cores. Experimental results show that SMC material has good 3D features, and great potential for application in rotational magnetic flux machines. Therefore, this study can assist magnetic material manufacturers in quality control and enable optimum design and thus shorten the development period of new high performance electrical machines.

#### ACKNOWLEDGMENT

This work is supported in part by the China Hebei

Provincial Natural Science Foundation under Grant No. E2008000051.

#### REFERENCES

- [1] H. Ahlers, J. D. Sievert, and Q. Qu, "Comparison of a single strip tester and Epstein Frame measurements," *J. Magn. Magn. Mater.*, vol. 26, no. 1-3, pp. 176-178, 1982.
- [2] J. Sievert, "Recent advances in the one- and two-dimensional magnetic measurement technique for electrical sheet steel," *IEEE Trans. Magn.*, vol. 26, no. 5, pp. 2553-2558, Sep. 1990.
- [3] M. Enokizono, T. Todaka, and S. Kanao, "Two-dimensional magnetic properties of silicon steel subjected to a rotating field," *IEEE Trans. Magn.*, vol. 29, no. 6, pp. 3550-3552, Nov. 1993.
- [4] J. G. Zhu and V. S. Ramsden, "Two dimensional measurement of magnetic field and core loss using a square specimen tester," *IEEE Trans. Magn.*, vol. 29, no. 6, pp. 2995-2997, Nov. 1993.
- [5] M. Enokizono, M. Morioka, K. Kawamura, and J. Sievert, "Distribution of two-dimensional magnetic properties in three-phase induction motor model core," *IEEE Trans. Magn.*, vol. 32, no. 5, pp. 4989-4991, Sep. 1996.
- [6] Y. G. Guo, J. G. Zhu, P. A. Watterson, and W. Wu, "Comparative study of 3D flux electrical machines with soft magnetic composite core," *IEEE Trans. Ind. Applicat.*, vol. 39, no. 6, pp. 1696-1703, 2003.
- [7] J. G. Zhu, J. J. Zhong, Z. W. Lin, and J. D. Sievert, "Measurement of magnetic properties under 3-D magnetic excitations," *IEEE Trans. Magn.*, vol. 39, no. 5, pp. 3429-3431, 2003.
- [8] Z. W. Lin and J. G. Zhu, "Three-dimensional magnetic properties of soft magnetic composite materials," *J. Magn. Magn. Mater.*, vol. 312, pp. 158-163, 2007.
- [9] Y. J. Li, J. G. Zhu, Q. X. Yang, Z. W. Lin, Y. G. Guo, and Y. Wang, "Magnetic measurement of soft magnetic composite material by an improved 3D tester with flexible excitation coils and novel sensing coils," *IEEE Trans. Magn.*, vol. 46, no. 6, pp. 1971-1974, Jun. 2010.
- [10] Reports of Höganäs AB, Sweden, 1997-2011, <http://www.hoganas.com>.
- [11] J. G. Zhu, J. J. Zhong, V. S. Ramsden, and Y. G. Guo, "Power losses of composite soft magnetic materials under two dimensional excitations," *J. Appl. Phys.*, vol. 85, no. 5, pp. 4403-4405, Apr. 15, 1999.
- [12] J. Kubik and P. Ripka, "Racetrack fluxgate sensor core demagnetization factor," *Sensors and Actuators A: Physical*, vol. 143, pp. 237-244, 2008.
- [13] Z. W. Lin, H. W. Lu, J. G. Zhu, J. J. Zhong, X. L. Wang, and S. Y. Ding, "Vector characterization of soft magnetic materials," *J. Appl. Phys.*, vol. 97, pp. 10R306-1-3, 2005.
- [14] J. J. Zhong, J. G. Zhu, Y. G. Guo, and Z. W. Lin, "Improved Measurement with 2D rotating fluxes considering effect of magnetization," *IEEE Trans. Magn.*, vol. 41, no. 10, pp. 3709-3711, Oct. 2005.
- [15] D. Jiles, *Introduction to Magnetism and Magnetic Materials*, 2nd ed. London: Chapman & Hall, 1998.